arXiv:1403.6041v1 [cond-mat.quant-gas] 24 Mar 2014

The Berry Curvature as a Magnetic Field in Momentum Space

Hannah M. Price, Tomoki Ozawa and Iacopo Carusotto
INO-CNR BEC Center and Dipartimento di Fisica, Università di Trento, I-38123 Povo, Italy

Artificial magnetism in momentum space can be engineered from the geometrical properties of energy bands. We show that the Berry curvature acts as a magnetic field in momentum space in the effective quantum Hamiltonian of a wide-range of systems. The effective Hamiltonian is equivalent to the textbook magnetic Hamiltonian, with the roles of momentum and position reversed. This duality has important implications for research into solid-state materials, spin-orbit coupling, ultracold gases and photonic systems. We propose a simple experiment that will demonstrate the advantages of this approach and that will also constitute the first realisation of magnetism on a torus.

The Hamiltonian of a charged particle in a magnetic field is a familiar and fundamental result in quantum mechanics[1]. In condensed matter physics, this Hamiltonian serves as a basic model for electrons in atoms and solids in the presence of magnetic fields. However, the textbook magnetic Hamiltonian is only one half of the full story. In this Hamiltonian, the roles of momentum and position are inherently asymmetric; the magnetic vector potential is a function of position that re-defines the relationship between the canonical and physical momenta. Here we show that the effective Hamiltonian of a very general class of systems is a magnetic Hamiltonian *in momentum space*. We build on ideas from the last sixty years[2–5] to discuss how the Berry curvature of an energy band acts as an artificial magnetic field with the roles of momentum and position reversed. Furthermore, we propose a simple experiment that will demonstrate the practical importance of understanding the effective magnetic Hamiltonian in momentum space. This general approach opens up new research avenues in diverse branches of physics, including ultracold gases, topological insulators, photonic systems, spin-orbit coupling and the mathematical physics of topological spaces.

Energy bands in momentum space are characterised not only by an energy spectrum, but also by important geometrical and topological properties. In recent years, these properties have been the subject of intense scientific research in many fields. Bands with nontrivial topological and geometrical properties are present in many solid-state materials[5], but thanks to important recent advances, they can also now be created in ultracold gases[6–9] and photonic systems[10–13]. The topological invariants of energy bands can be used to understand the quantisation of conductance in the quantum Hall effect[14] and to classify topological insulators[15, 16]. Topological invariants are closely related to local geometrical properties of energy bands, such as the Berry curvature[4, 5]. The Berry curvature of a band can be nonzero when time-reversal or inversion symmetry is broken[5], as, for example, for electrons in a magnetic field or with spin-orbit coupling. The Berry curvature has many direct physical consequences. For example, it plays an important role in the anomalous Hall effect[3, 17], the semiclassical dynamics of a wave packet[18] and the collective modes of an ultracold gas[19]. Berry phase effects have also been directly observed in graphene[20, 21] and bulk Rashba semiconductors[22].

Even though it was implicitly suggested very early[3, 4], the idea of the Berry curvature acting like a magnetic field in momentum space has so far been generally regarded as just a primitive analogy[5]. Here, we put this idea on a solid footing, demonstrating the remarkable power of this perspective and discussing some of its many consequences. We derive an effective magnetic Hamiltonian in momentum space which is of broad applicability and relevance. To illustrate our general discussion, we present two specific systems to which the effective magnetic Hamiltonian can be applied. First, we discuss two-dimensional (2D) Rashba spin-orbit coupling with a Zeeman field and an external potential, then we propose a simple experiment to study the Harper-Hofstadter model[23] with an additional harmonic trap. This experiment would be a natural extension of recent experiments in ultracold gases[8, 9], photonic systems[12] and solid-state superlattices[24].

The duality between the effective momentum space Hamiltonian and the textbook magnetic Hamiltonian is of great benefit to the study of both energy bands and magnetism. In particular, the energy bands of a two-dimensional periodic system are defined in the 2D Brillouin zone, which has the topology of a torus. In real space, the magnetic field through a torus is quantised, counting the number of magnetic monopoles contained inside. A torus in a real space magnetic field has long been of mathematical and theoretical interest[25, 26], but it has not previously been investigated experimentally. We show that this may now be possible, as the eigenstates of the Harper-Hofstadter model with a harmonic trap are momentum space Landau levels on a torus, for certain accessible parameter regimes. Alternatively, the effective Hamiltonian can be extended to energy bands with degeneracies, such as those in quantum spin Hall physics, graphene and topological insulators[15, 16]. The artificial gauge field in momentum space then has interesting properties; it is non-Abelian and may be connected to the Yang-Mills gauge field of high energy physics.

We begin with the general derivation of the effective magnetic Hamiltonian in momentum space. We start from the single-particle Hamiltonian, $\mathcal{H} = \mathcal{H}_0 + W$. The first part of the Hamiltonian, $\mathcal{H}_0$, is either translationally invariant or periodic in real space. For example, $\mathcal{H}_0$ could refer to an electron in a crystal, an atom with spin-orbit coupling, an ultracold atomic gas in an optical lattice or light in either a photonic crystal or a lattice of coupled resonators or waveguides. The second part of the Hamiltonian, W, is a weaker additional potential. This could be, for instance, an electric field for an electron or a harmonic trap or optical superlattice potential for atoms.

The eigenfunctions of $\mathcal{H}_0$ can be written as $|\chi_{n,\mathbf{p}}(\mathbf{r})\rangle = \frac{e^{i\mathbf{p}\cdot\mathbf{r}}}{\sqrt{V}}|n\mathbf{p}\rangle$, where $|n\mathbf{p}\rangle$ is the energy eigenstate for band index n and momentum $\mathbf{p}$, and V is a normalisation factor. If $\mathcal{H}_0$ is periodic, the eigenstate is the periodic Bloch function, $u_{n,\mathbf{k}}(\mathbf{r})$, and the momentum is the crystal momentum, $\mathbf{k}$, defined in the Brillouin zone (we take $\hbar = 1$ throughout). The normalisation, V, is the number of lattice sites, N. If instead $\mathcal{H}_0$ is translationally invariant, the eigenstate $|n\mathbf{p}\rangle$ is a position-independent wave function and V is the volume of the system. For simplicity, we focus on systems in 2D, although the extension to three dimensions is straightforward.

The energy bands are described by a band structure, $E_n(\mathbf{p})$, and have geometrical properties encoded in the Berry connection, $\mathcal{A}_n(\mathbf{p})$, and Berry curvature, $\Omega_n(\mathbf{p})$[4, 5]:

$$\mathcal{A}_n(\mathbf{p}) \equiv i\langle n\mathbf{p}|\frac{\partial}{\partial\mathbf{p}}|n\mathbf{p}\rangle, \tag{1}$$

$$\Omega_n(\mathbf{p}) \equiv \boldsymbol{\nabla}_\mathbf{p} \times \mathcal{A}_n(\mathbf{p}) \cdot \hat{\mathbf{z}}. \tag{2}$$

The additional potential, W, mixes different eigenstates, $|n\mathbf{p}\rangle$. The first example of this was investigated in 1959 to study the anomalous velocity of an electron in an electric field in a solid[3]. We build on these ideas to derive the effective Hamiltonian in a much more general, simple and modern context. We expand the eigenstates of the full Hamiltonian, $\mathcal{H}$, as:

$$|\Psi\rangle = \sum_n \sum_\mathbf{p} \psi_n(\mathbf{p})|\chi_{n,\mathbf{p}}\rangle, \tag{3}$$

where $\psi_n(\mathbf{p})$ are expansion coefficients. For a periodic $\mathcal{H}_0$, this sum is taken over the first Brillouin zone, otherwise, the sum runs over infinite momenta. We substitute into the Schrödinger equation, $i\frac{\partial}{\partial t}|\Psi\rangle = \mathcal{H}|\Psi\rangle$, and apply $\langle\chi_{n',\mathbf{p}'}|$, to obtain:

$$\begin{aligned} i\frac{\partial}{\partial t}\psi_n(\mathbf{p}) &= E_n(\mathbf{p})\psi_n(\mathbf{p}) \\ &+ \sum_n \sum_\mathbf{p} \langle\chi_{n',\mathbf{p}'}|W(\mathbf{r})|\chi_{n,\mathbf{p}}\rangle\psi_n(\mathbf{p}). \end{aligned} \tag{4}$$

To proceed, we expand $W(\mathbf{r})$ as a power series in $\mathbf{r}$, and repeatedly insert the completeness relation: $1 = \sum_n \sum_\mathbf{p} |\chi_{n,\mathbf{p}}\rangle\langle\chi_{n,\mathbf{p}}|$. Then we can use the identity:

$$\langle\chi_{n',\mathbf{p}'}|\mathbf{r}|\chi_{n,\mathbf{p}}\rangle = \delta_{\mathbf{p},\mathbf{p}'}\left(\delta_{n,n'}i\nabla_\mathbf{p} + i\langle n'\mathbf{p}'|\frac{\partial}{\partial\mathbf{p}}|n\mathbf{p}\rangle\right),$$

which we have generalised from a previously known result[2](Supplementary Information). We assume that the additional potential is sufficiently weak that it does not significantly mix energy bands and that the contribution from only one band n is non-negligible. A quantitative condition for this approximation will be discussed in the following. The effective quantum Hamiltonian in the single-band approximation is:

$$\tilde{\mathcal{H}} = E_n(\mathbf{p}) + W\left(i\nabla_\mathbf{p} + \mathcal{A}_n(\mathbf{p})\right). \tag{5}$$

The Berry connection enters like a magnetic vector potential in momentum space, modifying the physical position as $\mathbf{r} \to i\nabla_\mathbf{p} + \mathcal{A}_n(\mathbf{p})$, where $i\nabla_\mathbf{p} = \mathbf{R}$ is the canonical position[3, 17]. This is the reciprocal replacement to $\mathbf{p} \to -i\boldsymbol{\nabla}_\mathbf{r} + e\mathbf{A}(\mathbf{r})$; the correction of the physical momentum, $\mathbf{p}$, by a magnetic vector potential, $\mathbf{A}(\mathbf{r})$, where e is the electric charge[1]. In both cases, the canonical variable becomes gauge-dependent, while the physical variable remains independent of gauge.

The duality between momentum space magnetism and real space magnetism is also transparently demonstrated by comparing the effective Hamiltonian (5) to the textbook magnetic Hamiltonian of a charged particle:

$$\mathcal{H}' = \frac{\left(-i\boldsymbol{\nabla}_\mathbf{r} + eA(\mathbf{r})\right)^2}{2M} + V(\mathbf{r}), \tag{6}$$

for an external potential, $V(\mathbf{r})$, and particle mass, M. In particular, note that the roles of momentum and position are reversed. The energy bandstructure, $E_n(\mathbf{p})$, acts like the external potential $V(\mathbf{r})$, while $W\left(i\nabla_\mathbf{p} + \mathcal{A}_n(\mathbf{p})\right)$ corresponds to the "kinetic energy". The band index n could be a spin index in the magnetic analogy. When $W(\mathbf{r})$ is a harmonic trap, $W(\mathbf{r}) = \frac{1}{2}\kappa\mathbf{r}^2$, the effective momentum space Hamiltonian (5) is:

$$\tilde{\mathcal{H}} = E_n(\mathbf{p}) + \frac{\kappa\left(i\boldsymbol{\nabla}_\mathbf{p} + \mathcal{A}_n(\mathbf{p})\right)^2}{2}. \tag{7}$$

Comparing with equation (6), we see that the inverse trapping strength, κ^{-1}, is equivalent to the mass of the particle, M. Different types of external potential, $W(\mathbf{r})$, are equivalent to different energy-momentum relationships in the real space magnetic Hamiltonian.

The effective Hamiltonian (5) may also be generalised to systems such as graphene and topological insulators. Instead of making a single band approximation, we could keep a sub-space of degenerate or nearly degenerate bands (Supplementary Information). The effective momentum space magnetic field then has a non-Abelian gauge structure[27].

The anomalous velocity[3] and semiclassical equations of motion[18] follow straightforwardly from Hamilton's equations: $\dot{\mathbf{R}} = \frac{\partial \tilde{\mathcal{H}}}{\partial \mathbf{p}}$ and $\dot{\mathbf{p}} = -\frac{\partial \tilde{\mathcal{H}}}{\partial \mathbf{R}}$. The velocity will be:

$$\dot{\mathbf{r}} = \frac{\partial E_n(\mathbf{p})}{\partial \mathbf{p}} + \frac{\partial W}{\partial \mathbf{r}} \times \Omega_n(\mathbf{p}), \tag{8}$$

provided that we can either approximate the potential, $W(\mathbf{r})$ as a locally uniform force[3], or approximate the Berry curvature as locally constant in momentum space.

The contribution of the Berry curvature to the velocity is analogous to the Lorentz force in magnetism. This has important experimental consequences, for example, for a particle with 2D Rashba spin-orbit coupling in a Zeeman field[5, 19, 28]. This model is relevant for real materials[28], as well as ultracold gases, where there is great interest in creating 2D artificial spin-orbit coupling[29]. The basic Hamiltonian is:

$$\mathcal{H}_0 = \frac{\mathbf{p}^2}{2M} + \lambda(p_x\hat{\sigma}_y - p_y\hat{\sigma}_x) - \Delta\hat{\sigma}_z, \tag{9}$$

where $\hat{\sigma}_{x,y,z}$ are the Pauli matrices, Δ is the Zeeman field and λ is the spin-orbit coupling strength. The Hamiltonian, $\mathcal{H}_0$, has two energy bands, $E_\pm(\mathbf{p}) = \frac{p^2}{2M} \pm \sqrt{\lambda^2 p^2 + \Delta^2}$, which are non-degenerate provided that Δ is non-zero. The Berry curvature is[28]:

$$\Omega_\pm(\mathbf{p}) = \mp\frac{\lambda^2\Delta}{2(\lambda^2 p^2 + \Delta^2)^{3/2}}. \tag{10}$$

With an external harmonic potential, $W(\mathbf{r}) = \frac{1}{2}\kappa\mathbf{r}^2$, a particle in the lowest band can be described by the effective Hamiltonian (7). For $\lambda^2 M/\Delta < 1$, the lowest band has a single minimum at $\mathbf{p} = 0$. For a gas condensed at this minimum, the Berry curvature acts as a momentum space magnetic field, splitting the dipole mode frequencies of a trapped ultracold gas[19] (Supplementary Information). The splitting of the dipole modes can be large, and would be directly observable within current experimental capabilities[19].

While the Berry curvature considered in equation (5) is a local property of the energy band, the global topology of the momentum space can also play an important role. In the Rashba model discussed above, the basic Hamiltonian, $\mathcal{H}_0$, is translationally invariant and the momentum $\mathbf{p}$ is continuous and unconstrained. However, when $\mathcal{H}_0$ is periodic, the momentum is defined over the Brillouin zone, which has the topology of a torus.

It is well known that real space magnetism on a torus has many interesting properties, such as the quantisation of magnetic flux due to the presence of magnetic monopoles. In the analogy with magnetism, this is equivalent to the quantisation of the Berry curvature, integrated over the entire Brillouin Zone, in units of the Chern number: the topological invariant underlying the quantum Hall effect[14]. In the following, we propose a simple experiment to study magnetism on a torus experimentally for the first time. We investigate the eigenstates of the Harper-Hofstadter Hamiltonian[23] with an external harmonic trap; such an experiment would be a natural extension of recent advances[8, 9, 12, 24].

In the Harper-Hofstadter model, a particle hops on a 2D lattice in a perpendicular magnetic field, $\boldsymbol{B} = B\hat{\mathbf{z}}$. Choosing the magnetic vector potential in the Landau gauge, $\mathbf{A}(\mathbf{r}) = Bx\hat{\mathbf{y}}$, the tight-binding Hamiltonian with a harmonic trap is:

$$\mathcal{H} = \mathcal{H}_0 + \frac{1}{2}\kappa a^2 \sum_{m,n}(m^2+n^2)\hat{a}^\dagger_{m,n}\hat{a}_{m,n},$$
$$\mathcal{H}_0 = -J\sum_{m,n}\left(\hat{a}^\dagger_{m+1,n}\hat{a}_{m,n} + e^{i\phi}\hat{a}^\dagger_{m,n+1}\hat{a}_{m,n}\right) + \text{h.c.} \tag{11}$$

where $\mathcal{H}_0$ is the Harper-Hofstadter Hamiltonian, J is the hopping amplitude, a is the lattice spacing and the $\hat{a}^\dagger_{m,n}$ ($\hat{a}_{m,n}$) operators create (annihilate) a particle at lattice site (m,n). The hopping along $\hat{\mathbf{y}}$ is modified by a complex phase $\phi = 2\pi\alpha ma$, where α is the number of magnetic flux quanta per plaquette of the lattice.

Without a harmonic trap, there is just the Harper-Hofstadter Hamiltonian, $\mathcal{H}_0$, and the behaviour is governed by the value of α. For rational values of $\alpha = p/q$, the tight-binding band splits into q magnetic sub-bands. The energy spectrum of the Harper-Hofstadter Hamiltonian is the well-known Hofstadter butterfly[23]. The magnetic vector potential, $\mathbf{A}(\mathbf{r})$, is not periodic, and the usual translation operators do not commute with $\mathcal{H}_0$[18]. Bloch's theorem can be applied only when we define new magnetic translation operators which do commute with $\mathcal{H}_0$. For these to also commute amongst themselves, we define a larger magnetic unit cell of q plaquettes, containing an integer number of magnetic flux quanta. Then the Bloch states are *magnetic* Bloch states and the crystal momentum, $\mathbf{k}$, is defined within the *magnetic* Brillouin zone (MBZ): $-\pi/a < k_y \leq \pi/a$ and $-\pi/qa < k_x \leq \pi/qa$ (for a magnetic unit cell of q plaquettes along $\hat{\mathbf{x}}$) [18] .

We numerically diagonalise the full Hamiltonian, $\mathcal{H}$, with the harmonic trap (11). The energy spectrum is shown in Figure 1 for low energies as a function of magnetic flux, α. This was calculated for $\kappa a^2/J = 0.02$ on a lattice of 21 by 21 sites. The weak harmonic potential splits the Harper-Hofstatder bands into a complicated structure first noted in Ref. 30. Here we show that these eigenstates can be understood through the analogy between Berry curvature and magnetism.

When the single-band approximation is valid, the physics of the full system (11) is described by the effective momentum space Hamiltonian (5). We focus on the regime $\alpha = 1/q \ll 1$ so that we can make two further simplifications. Firstly, with decreasing $\alpha = 1/q$, the bands flatten compared to the hopping energy J. If the bandwidth is much smaller than κa^2, we can assume $E_n(\mathbf{k}) \simeq E_n$. The effect of the band structure is then only

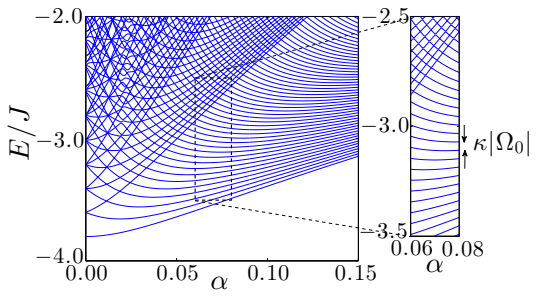

FIG. 1. **The Low Energy Spectrum of the Harper-Hofstadter Model with a Harmonic Potential**. The numerical diagonalisation of Eq. 11, for a harmonic trapping strength of $\kappa a^2/J = 0.02$ and a lattice of 21 by 21 sites. (These numerical results were first obtained in Ref. 30, but a complete interpretation was not provided.) As shown in the inset, the harmonic trap splits the lowest Hofstadter band into a ladder of toroidal Landau levels, with an equal energy spacing of $\kappa|\Omega_0| = \kappa a^2/2\pi\alpha$. At increasing energies, higher bands are also split into ladders of toroidal Landau levels. As $\alpha \to 0$, the effective Hamiltonian breaks down and the states are those of a 2D simple harmonic oscillator on a lattice[30].

to shift the overall energy. Secondly, when $\alpha = 1/q$ and q is odd, the Chern number of each band, except the middle band, is -1. For $\alpha \ll 1$, the Berry curvature of these bands is increasingly uniform, $\Omega_n(\mathbf{k}) \simeq \Omega_n$. The uniform value of the Berry curvature, $|\Omega_0| = a^2/(2\pi\alpha)$, is found by noting that the Chern number: $\mathcal{C}_0 = \frac{1}{2\pi}\Omega_0 A_{\rm BZ} = -1$, where $A_{\rm BZ} = (2\pi)^2/qa^2$ is the area of the MBZ[19]. Therefore for $\alpha = 1/q \ll 1$, the effective Hamiltonian describes a particle in a uniform magnetic field in momentum space, with an additional overall energy shift.

The eigenstates of a particle in a real space uniform magnetic field are the infinitely degenerate Landau levels[1]. Introducing periodic boundary conditions restricts the particle to the surface of a torus[25, 26]. Toroidal Landau levels are superpositions of the infinitely degenerate Landau levels such that the boundary conditions are satisfied. From the duality between momentum space magnetism and real space magnetism, we can deduce the properties of toroidal Landau levels in the magnetic Brillouin zone. The energy is unaffected by topology and is given by the well-known Landau level spectrum:

$$\mathcal{E}_n = (\beta + \frac{1}{2})\kappa|\Omega_n|, \tag{12}$$

where $\beta = 0, 1, 2...$ is the Landau level quantum number and $\kappa|\Omega_n|$ is the analogue of the cyclotron frequency, $\omega_c = e|B|/M$. The degeneracy of toroidal Landau levels is finite and equal to the quantised number of magnetic flux quanta piercing the torus[25]. Counting the degeneracy of such states may therefore provide another experimental tool to directly measure the Chern number of non-degenerate energy bands.

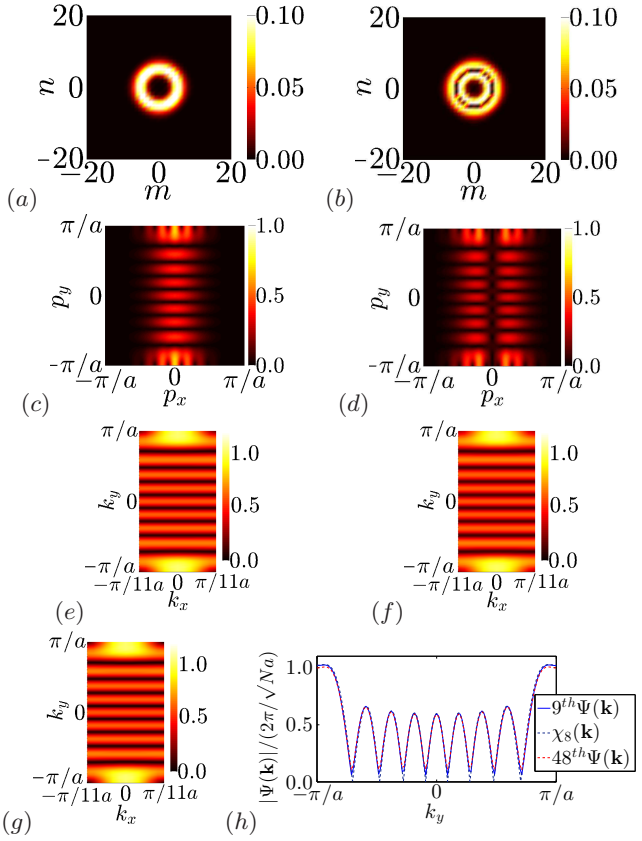

FIG. 2. **Identifying Landau Levels on a Torus**. (a)&(b) The wave function, $|\psi(\mathbf{r})|$, in units of a^{-1}. (c)&(d) The absolute value of the Fourier transform of $\psi(\mathbf{r})$, in units of $(2\pi/\sqrt{N}a)^{-1}$, in the full Brillouin zone (see Supplementary Information for details). N is the number of lattice sites over which the numerical calculation was performed. (e)&(f) The wave function, $|\psi(\mathbf{k})|$, in the magnetic Brillouin zone, in units of $(2\pi/\sqrt{N}a)^{-1}$. The left (right) column is the 9th (48th) lowest eigenstate of Eq. (11) for $\alpha = 1/11$, $\kappa a^2/J = 0.02$ and $N = (133)^2$. (g)&(h) Comparison with theory. Respectively, the $\beta = 8$ toroidal Landau level with $|\Omega| = a^2/(2\pi\alpha)$ (Eq. 13) and a quantitative comparison of a cut along $k_x = 0$ taken from (e), (f) &(g).

As shown in the inset of Fig. 1, the lowest Harper-Hofstadter band is split into a ladder of equispaced states. The energy spacing of these states is in excellent agreement with Eq. 12 where $|\Omega_0| = a^2/(2\pi\alpha)$. The result was also noted in Ref. 30 but its origin was not discussed there. These states are non-degenerate reflecting the Chern number of the lowest band. Similar behaviour is also observed for $p \neq 1$; this will be discussed in a future publication. Note that, as shown in Fig. 1, this result only holds for sufficiently large α such that the single band approximation is valid. For smaller values of α, one recovers the energy spacing of a 2D simple harmonic oscillator on a tight-binding lattice[30].

Looking again at the inset of Fig. 1, one notes that at higher energies a second ladder of states cuts diagonally

across the first ladder. These states can be identified as toroidal Landau levels in the second lowest Harper-Hofstadter band. The single band approximation requires that $\kappa a^2 \ll (E_n - E_{n'})$. This is easily fulfilled for our choice of parameters: the splitting of the two lowest bands, for example, is $(E_1 - E_0) \simeq J$ for $\alpha = 1/11$ without a harmonic trap. The effective Hamiltonian applies to each band separately, without inter-band coupling. Increasing the energy, Landau levels of other bands also appear. However, our assumptions eventually break down: the inter-band transition energy decreases, and the Berry curvature and band structure become increasingly non-uniform.

We can also compare the form of the numerical eigenstates with those of theoretical Landau levels on a torus[26]. In the magnetic Brillouin zone, when $|\mathcal{C}_n| = 1$, the states are:

$$\chi_\beta(\mathbf{k}) = \mathcal{N}_\beta^{l_{\Omega_n}} \sum_{j=-\infty}^{\infty} e^{ik_y ja} e^{-(k_x - jal_{\Omega_n}^2)^2/2l_{\Omega_n}^2} \times H_\beta(k_x/l_{\Omega_n} - jal_{\Omega_n}), \quad (13)$$

where H_β are Hermite polynomials and $\mathcal{N}_\beta^{l_{\Omega_n}}$ is a normalisation constant (Supplementary Information). The characteristic momentum scale is $l_{\Omega_n} = \sqrt{1/|\Omega_n|}$, the analogue to the "magnetic length". Like a real space magnetic vector potential, the Berry connection is gauge-dependent. In writing down this wave function, we chose the Landau gauge for the momentum space Berry connection, $\mathcal{A}_n(\mathbf{k}) = |\Omega_n| k_x \hat{\mathbf{k}}_y$, although we only directly compare quantities that are independent of this gauge-choice with numerics. The excellent agreement between Landau levels on a torus and the numerical eigenstates is shown in Fig. 2, for the 9th and 48th numerical states. These correspond to the $\beta = 8$ toroidal Landau level in the first and second Harper-Hofstadter bands respectively.

Our simple proposal is well suited to experiments as the Landau levels observed are remarkably robust. According to our numerics, the basic features of the lowest energy toroidal Landau levels survive for magnetic flux up to $\alpha = 1/5$ and for $\kappa a^2/J \simeq 0.5$. This gives a large parameter regime over which the properties of the effective magnetic Hamiltonian may be investigated. Importantly, these results are also very insensitive to lattice size, due to strong localisation of the low energy eigenstates in real space (Fig. 2). This is because toroidal Landau levels are delocalised in momentum space, varying over a large characteristic momentum-scale, l_{Ω_n}. Therefore, experiments can be performed for very small lattices, which is a key technical advantage. Experimentally, a harmonic trap can be added straightforwardly to an ultracold gas by using additional laser beams and/or magnetic fields. The eigenstates of the system can be probed directly in time-of-flight measurements of the momentum distribution. In photonic systems, a harmonic potential might be created by letting the cavity size vary in space, while the momentum space wave function is measured in the far-field emitted light[12]. It is important to remember that the eigenstates depend on the magnetic gauge chosen for the Harper-Hofstadter Hamiltonian (11). However, in both ultracold gases and photonic systems, there is a preferential magnetic gauge choice inherent in the experimental set-up[8, 9, 12].

The magnetic Hamiltonian in momentum space is the counterpart to an important textbook result. It is also applicable to many systems of current experimental interest. These also include quantum spin Hall models, graphene and topological insulators, where the gauge field becomes non-Abelian. In the future, the analogy between magnetism and energy bands should open up many new avenues of research. It also raises many interesting open questions concerning the role of interactions and the possibility of momentum-space electrodynamics.

We are grateful to N. R. Cooper for helpful comments and to P. Ghiggini for mathematical support. This work was partially funded by ERC through the QGBE grant and by the Autonomous Province of Trento, Call "Grandi Progetti 2012," project "On silicon chip quantum optics for quantum computing and secure communications - SiQuro".

[1] L. D. Landau and L. M. Lifshitz, *Quantum Mechanics, Third Edition: Volume 3*, 3rd ed. (Butterworth-Heinemann, Oxford, 1958).
[2] R. Karplus and J. M. Luttinger, Phys. Rev. **95**, 1154 (1954).
[3] E. N. Adams and E. I. Blount, J. Phys. Chem. Solids **10**, 286 (1959).
[4] M. V. Berry, Proc. R. Soc. London, Ser. A **392**, 45 (1984).
[5] D. Xiao, M.-C. Chang, and Q. Niu, Rev. Mod. Phys. **82**, 1959 (2010).
[6] L. Tarruell, D. Greif, T. Uehlinger, G. Jotzu, and T. Esslinger, Nature **483**, 302 (2012).
[7] J. Struck *et al.*, Nature Phys. **9**, 738 (2013).
[8] M. Aidelsburger *et al.*, Phys. Rev. Lett. **111**, 185301 (2013).
[9] H. Miyake, G. A. Siviloglou, C. J. Kennedy, W. C. Burton, and W. Ketterle, Phys. Rev. Lett. **111**, 185302 (2013).
[10] Z. Wang, Y. Chong, J. D. Joannopoulos, and M. Soljačić, Nature **461**, 772 (2009).
[11] M. C. Rechtsman *et al.*, Nature **496**, 196 (2013).
[12] M. Hafezi, S. Mittal, J. Fan, A. Migdall, and J. M. Taylor, Nature Photon. **7**, 1001 (2013).
[13] T. Jacqmin *et al.*, Phys. Rev. Lett. **112**, 116402 (2014).
[14] D. J. Thouless, M. Kohmoto, M. P. Nightingale, and M. den Nijs, Phys. Rev. Lett. **49**, 405 (1982).
[15] M. Z. Hasan and C. L. Kane, Rev. Mod. Phys. **82**, 3045 (2010).
[16] X.-L. Qi and S.-C. Zhang, Rev. Mod. Phys. **83**, 1057 (2011).

[17] N. Nagaosa, J. Sinova, S. Onoda, A. H. MacDonald, and N. P. Ong, Rev. Mod. Phys. **82**, 1539 (2010).
[18] M.-C. Chang and Q. Niu, Phys. Rev. Lett. **75**, 1348 (1995).
[19] H. M. Price and N. R. Cooper, Phys. Rev. Lett. **111**, 220407 (2013).
[20] K. S. Novoselov *et al.*, Nature **438**, 197 (2005).
[21] Y. B. Zhang, Y. W. Tan, H. L. Stormer, and P. Kim, Nature **438**, 201 (2005).
[22] H. Murakawa *et al.*, Science **342**, 1490 (2013).
[23] D. R. Hofstadter, Phys. Rev. B **14**, 2239 (1976).
[24] C. R. Dean *et al.*, Nature **497**, 598 (2013).
[25] J. K. Jain, *Composite Fermions* (Cambridge University Press, Cambridge, 2007).
[26] M. H. Al-Hashimi and U.-J. Wiese, Ann. Phys. **324**, 343 (2009).
[27] F. Wilczek and A. Zee, Phys. Rev. Lett. **52**, 2111 (1984).
[28] D. Culcer, A. MacDonald, and Q. Niu, Phys. Rev. B **68**, 045327 (2003).
[29] V. Galitski and I. B. Spielman, Nature **494**, 49 (2013).
[30] A. R. Kolovsky, F. Grusdt, and M. Fleischhauer, Phys. Rev. A **89**, 033607 (2014).

arXiv:1403.6041v1 [cond-mat.quant-gas] 24 Mar 2014

SUPPLEMENTARY INFORMATION: THE BERRY CURVATURE AS A MAGNETIC FIELD IN MOMENTUM SPACE

Derivation of The Effective Hamiltonian for an External Harmonic Trap

Here we explicitly derive the effective Hamiltonian for an external harmonic trap, $W(\mathbf{r}) = \frac{1}{2}\kappa\mathbf{r}^2$. We begin from the Schrödinger equation, expanded in terms of the eigenstates of $\mathcal{H}_0$:

$$i\frac{\partial}{\partial t}\psi_n(\mathbf{p}) = E_n(\mathbf{p})\psi_n(\mathbf{p}) + \sum_n \sum_{\mathbf{p}} \frac{\kappa}{2}\langle\chi_{n',\mathbf{p}'}|\mathbf{r}^2|\chi_{n,\mathbf{p}}\rangle\psi_n(\mathbf{p}). \tag{1}$$

In the last line, we insert the completeness relation of Bloch states, $1 = \sum_n \sum_{\mathbf{p}} |\chi_{n,\mathbf{p}}\rangle\langle\chi_{n,\mathbf{p}}|$:

$$i\frac{\partial}{\partial t}\psi_n(\mathbf{p}) = E_n(\mathbf{p})\psi_n(\mathbf{p}) + \frac{\kappa}{2}\sum_{n,n''}\sum_{\mathbf{p},\mathbf{p}''}\langle\chi_{n',\mathbf{p}'}|\mathbf{r}|\chi_{n'',\mathbf{p}''}\rangle\langle\chi_{n'',\mathbf{p}''}|\mathbf{r}|\chi_{n,\mathbf{p}}\rangle\psi_n(\mathbf{p}) \tag{2}$$

Now that the Schrödinger equation is in this form, we can apply an identity to replace terms of the type: $\langle\chi_{n',\mathbf{p}'}|\mathbf{r}|\chi_{n,\mathbf{p}}\rangle$. This identity is a generalised version of a result originally due to Karplus and Luttinger[1]. The derivation is as follows:

$$\begin{aligned}
\langle\chi_{n',\mathbf{p}'}|\mathbf{r}|\chi_{n,\mathbf{p}}\rangle &= \int d^2\mathbf{r}\; w^*_{n',\mathbf{p}'}(\mathbf{r})e^{-i\mathbf{p}'\cdot\mathbf{r}}\mathbf{r}e^{i\mathbf{p}\cdot\mathbf{r}}w_{n,\mathbf{p}}(\mathbf{r}) \\
&= -i\int d^2\mathbf{r} w^*_{n',\mathbf{p}'}(\mathbf{r})e^{-i\mathbf{p}'\cdot\mathbf{r}}\left(\boldsymbol{\nabla}_{\mathbf{p}}e^{i\mathbf{p}\cdot\mathbf{r}}\right)w_{n,\mathbf{p}}(\mathbf{r}) \\
&= -i\nabla_{\mathbf{p}}\left[\int d^2\mathbf{r}\; e^{-i(\mathbf{p}'-\mathbf{p})\cdot\mathbf{r}}w^*_{n',\mathbf{p}'}(\mathbf{r})w_{n,\mathbf{p}}(\mathbf{r})\right] + i\int d^2\mathbf{r}\; e^{-i(\mathbf{p}'-\mathbf{p})\cdot\mathbf{r}}w^*_{n',\mathbf{p}'}(\mathbf{r})\nabla_{\mathbf{p}}w_{n,\mathbf{p}}(\mathbf{r}),
\end{aligned} \tag{3}$$

where $w_{n,\mathbf{p}}(\mathbf{r}) = \langle\mathbf{r}|n\mathbf{p}\rangle$. If $\mathcal{H}_0$ is periodic, the momentum is the crystal momentum, $\mathbf{k}$ and $w_{n,\mathbf{p}}(\mathbf{r}) = u_{n,\mathbf{k}}(\mathbf{r})$. As the Bloch functions are periodic, the last integral will vanish[1] unless $\mathbf{k} = \mathbf{k}'$. Otherwise, if $\mathcal{H}_0$ is not periodic, then $w_{n,\mathbf{p}}(\mathbf{r}) = w_{n,\mathbf{p}}$ is independent of position. Then the last integral will vanish unless $\mathbf{p} = \mathbf{p}'$. Using the orthonormality of the eigenfunctions, and integrating the derivative of the delta function by parts, we obtain the identity:

$$\langle\chi_{n',\mathbf{p}'}|\mathbf{r}|\chi_{n,\mathbf{p}}\rangle = \delta_{\mathbf{p},\mathbf{p}'}\left(\delta_{n,n'}i\nabla_{\mathbf{p}'} + i\langle n'\mathbf{p}'|\frac{\partial}{\partial\mathbf{p}}|n\mathbf{p}\rangle\right). \tag{4}$$

We can recognise the last term as the generalised non-Abelian Berry connection[2]: $\mathcal{A}_{n',n}(\mathbf{p}) = i\langle n'\mathbf{p}|\frac{\partial}{\partial\mathbf{p}}|n\mathbf{p}\rangle$. Substituting the identity into the Schrödinger equation, we find:

$$i\frac{\partial}{\partial t}\psi_n(\mathbf{p}) = E_n(\mathbf{p})\psi_n(\mathbf{p}) + \frac{\kappa}{2}\sum_{n,n''}\left(\delta_{n',n''}i\nabla_{\mathbf{p}} + \mathcal{A}_{n',n''}(\mathbf{p})\right)\cdot\left(\delta_{n'',n}i\nabla_{\mathbf{p}} + \mathcal{A}_{n'',n}(\mathbf{p})\right)\psi_n(\mathbf{p}). \tag{5}$$

If we assume that the external potential does not significantly mix energy bands, we can make a single band approximation. The Schrödinger equation then reduces to:

$$i\frac{\partial}{\partial t}\psi_n(\mathbf{p}) = \left[E_n(\mathbf{p}) + \frac{\kappa}{2}\left(i\nabla_{\mathbf{p}} + \mathcal{A}_n(\mathbf{p})\right)^2\right]\psi_n(\mathbf{p}). \tag{6}$$

We note that the Schrödinger equation could equally have been restricted to a sub-space of degenerate or nearly degenerate bands that are well-separated in energy from other bands. Then the sums in Eq. 5 only run over this sub-space of bands. The corresponding Berry curvature would be[2]:

$$\mathcal{F}(\boldsymbol{p}) \equiv \boldsymbol{\nabla}_p \times \mathcal{A}(\boldsymbol{p}) - i\mathcal{A}(\boldsymbol{p}) \times \mathcal{A}(\boldsymbol{p}) \tag{7}$$

which has a non-Abelian gauge structure[3]. This may be related to the Yang-Mills gauge field in high energy physics[4]. Physically, an energy band Hamiltonian containing the non-Abelian Berry connection, $\mathcal{A}_{n',n}(\mathbf{p})$, may describe quantum spin Hall models, graphene or topological insulators[5, 6] in additional potentials.

The Dipole Mode for a Particle with 2D Rashba Spin-Orbit Coupling in a Zeeman Field

Reference 7 showed that the Berry curvature can cause significant modifications to the collective modes of a trapped Bose-Einstein condensate. Here, we present a simple discussion of their result for a particle with 2D Rashba spin-orbit coupling in a Zeeman field and a weak external harmonic trap[7] to underline the importance of momentum space magnetic fields in the equations of motion. The single particle Hamiltonian of a particle with 2D Rashba spin-orbit coupling in a Zeeman field and a harmonic trap is:

$$\mathcal{H} = \mathcal{H}_0 + W = \frac{\mathbf{p}^2}{2M} + \lambda(p_x\hat{\sigma}_y - p_y\hat{\sigma}_x) - \Delta\hat{\sigma}_z + \frac{1}{2}\kappa(\mathbf{x}^2 + \mathbf{y}^2), \tag{8}$$

where $\hat{\sigma}_{x,y,z}$ are the Pauli matrices and λ is the spin-orbit coupling strength. When $\kappa = 0$, the Hamiltonian has two energy bands, $E_\pm(\mathbf{p}) = \frac{p^2}{2M} \pm \sqrt{\lambda^2 p^2 + \Delta^2}$. When $\lambda^2 M/\Delta < 1$, the lowest band has a single minimum at $\mathbf{p} = 0$. The behaviour of a particle at this minimum is characterised by the effective mass and the Berry curvature:

$$M^* = \frac{1}{(\partial^2 E_-/\partial^2 \mathbf{p})}\bigg|_{\mathbf{p}=0} = \frac{M}{1 - \frac{\lambda^2 M}{\Delta}}, \qquad \Omega = \frac{\lambda^2\Delta}{2(\lambda^2 p^2 + \Delta^2)^{3/2}}\bigg|_{\mathbf{p}=0} = \frac{\lambda^2}{2\Delta^2}. \tag{9}$$

Within this description, the Berry curvature is constant and the single particle equations of motion follow straightforwardly from the momentum space magnetic Hamiltonian as:

$$\dot{\mathbf{r}} = \frac{\partial E_-(\mathbf{p})}{\partial \mathbf{p}} + \kappa\,(\mathbf{r} \times \hat{\mathbf{z}})\,\Omega, \qquad \dot{\mathbf{p}} = -\kappa\mathbf{r}. \tag{10}$$

Approximating the dispersion as quadratic, these equations can be combined to give[7]:

$$\ddot{\mathbf{r}} = -\frac{\kappa\mathbf{r}}{M^*} + \kappa\,(\dot{\mathbf{r}} \times \hat{\mathbf{z}})\,\Omega. \tag{11}$$

Interactions do not affect the dipole mode of a gas in a quadratic band minimum[7]; this mode is a "sloshing" of the centre of mass: $\mathbf{r} = (\mathbf{x} \pm i\mathbf{y})e^{-i\omega t}$. The dipole mode frequencies of an ultracold gas therefore follow from the single particle equation of motion (11) as[7]:

$$\omega = \mp\frac{\kappa\Omega}{2} + \frac{1}{2}\sqrt{(\kappa\Omega)^2 + \frac{4\kappa}{M^*}}. \tag{12}$$

Without Berry curvature, the dipole modes are degenerate[8]. The presence of the effective momentum space magnetic field splits these modes by $\kappa\Omega$, as is the case for electrons in a harmonic trap in the presence of a magnetic field. This splitting can be large and within current experimental capabilities[7]. (A more general discussion of the effects of Berry curvature on collective modes of a gas with interactions is also presented in Ref. 7.)

Extracting the Eigenstates in the Magnetic Brillouin Zone from the Numerics of the Harper-Hofstadter Model with a Harmonic Trap

Here we show how the eigenstates of the Harper-Hofstadter Hamiltonian with a harmonic trap can be obtained numerically in the magnetic Brillouin zone. We diagonalise the Hamiltonian to find the numerical energy eigenstates in real space:

$$|\Psi\rangle = \sum_{m,n} \psi(m,n) a^\dagger_{m,n}|0\rangle, \tag{13}$$

where $\psi(m,n)$ are the eigenfunction coefficients for each lattice site. (The eigenstates are normalised to a lattice of area Na^2.) To observe toroidal Landau levels, this wave-function must be transformed into the MBZ. We first Fourier transform the real space wave function, to find:

$$|\Psi\rangle = \sum_{p_x,p_y} \psi(p_x,p_y) a^\dagger_{p_x,p_y}|0\rangle, \tag{14}$$

where $\mathbf{p} = (p_x, p_y)$ is the crystal momentum in the *full* Brillouin zone: $-\pi/a < \mathbf{p} \leq \pi/a$.

We note that the magnetic Brillouin zone is defined from the Harper-Hofstadter Hamiltonian without a harmonic trap[9, 10]. For clarity, we demonstrate this by taking the Fourier transform of the lattice creation and annihilation operators:

$$\hat{a}_{m,n} = \sum_{p_x,p_y} e^{ip_x ma + ip_y na} \hat{a}_{p_x,p_y},$$
$$\hat{a}^\dagger_{m,n} = \sum_{p_x,p_y} e^{-ip_x ma - ip_y na} \hat{a}^\dagger_{p_x,p_y}, \tag{15}$$

and substituting them into $\mathcal{H}_0$. After simplifying the algebra, the Harper-Hofstadter Hamiltonian in the full Brillouin zone becomes[11]:

$$\mathcal{H}_0 = \sum_{p_x,p_y} [-2J\cos(p_x a)\hat{a}^\dagger_{p_x,p_y}\hat{a}_{p_x,p_y} - J(e^{-ip_y a}\hat{a}^\dagger_{p_x+2\pi\alpha/a,p_y}\hat{a}_{p_x,p_y} + e^{ip_y}\hat{a}^\dagger_{p_x-2\pi\alpha/a,p_y}\hat{a}_{p_x,p_y})]. \tag{16}$$

This is not diagonal in the full Brillouin zone, as p_x is mixed with $p_x + 2\pi\alpha/a$ and $p_x - 2\pi\alpha/a$. However, the Hamiltonian can be made diagonal, by defining a new variable: $k_x = p_x + j2\pi\alpha/a$, where j is an integer. For $\alpha = 1/q$, $\mathbf{G} = 2\pi\alpha/a\hat{k}_x$ is a magnetic reciprocal lattice vector for the unit cell discussed in the text, and $\mathbf{k}$ is the magnetic crystal momentum. Note that the choice of the new variable, $\mathbf{k}$, followed naturally from the magnetic gauge of $\mathcal{H}_0$. We have deliberately picked the magnetic unit cell for which: $\mathbf{k} = \mathbf{p} + j\mathbf{G}$. (For other choices of magnetic unit cell, this relation would not generally take this simple form.) We can then write:

$$|\chi_{n,\mathbf{k}}\rangle = \sum_{\mathbf{p}} U_{n,\mathbf{k}}(\mathbf{p})\hat{a}^\dagger_{\mathbf{p}}|0\rangle, \tag{17}$$

where $U_{n,\mathbf{k}}(\mathbf{p})$ is a unitary matrix that transforms eigenstates between the full and magnetic Brillouin zone. This matrix only has non-zero values for $\mathbf{p} = \mathbf{k} - j\mathbf{G}$. Taking the inverse of Eq. 17 and applying it to Eq. 14, we have:

$$|\Psi\rangle = \sum_{n,\mathbf{k},\mathbf{p}} U^*_{n,\mathbf{k}}(\mathbf{p})\psi(\mathbf{p})|\chi_{n,\mathbf{k}}\rangle$$
$$= \sum_{n,\mathbf{k}} \psi_n(\mathbf{k})|\chi_{n,\mathbf{k}}\rangle, \tag{18}$$

where $\psi_n(\mathbf{k})$ are the wave function coefficients in the magnetic Brillouin zone. Then it follows that:

$$\sum_n |\psi_n(\mathbf{k})|^2 = \sum_j |\psi(\mathbf{p} = \mathbf{k} - j\mathbf{G})|^2. \tag{19}$$

If we make the single band approximation, and assume that $\psi_n(\mathbf{k})$ is only non-negligible in one band, we obtain $|\psi_n(\mathbf{k})|^2 = \sum_j |\psi(\mathbf{p} = \mathbf{k} - j\mathbf{G})|^2$. This relationship is used to calculate the numerical wave function in the magnetic Brillouin zone in the main text & below in Fig. S1.

Further Details for Toroidal Landau Levels

Here we give further details and examples of toroidal Landau levels. As stated in the main text, for $|\mathcal{C}_n| = 1$, these have the form:

$$\chi_\beta(\mathbf{k}) = \mathcal{N}^{l_{\Omega_n}}_\beta \sum_{j=-\infty}^{\infty} e^{ik_y ja} e^{-(k_x - jal^2_{\Omega_n})^2/2l^2_{\Omega_j}} H_\beta(k_x/l_{\Omega_n} - jal_{\Omega_n}) \tag{20}$$

translated from the theoretical Landau levels of a particle on a real space torus[12]. We note that the form of these levels depends on the Chern number and the dimensions of the magnetic Brillouin zone. The wave function obeys periodic boundary conditions and the "solenoid fluxes" are zero. The normalisation constant is:

$$\mathcal{N}^{l_{\Omega_n}}_\beta = \left(\frac{\sqrt{2/q}}{(2^\beta \beta! \times 2\pi l^2_{\Omega_n})}\right)^{1/2}. \tag{21}$$

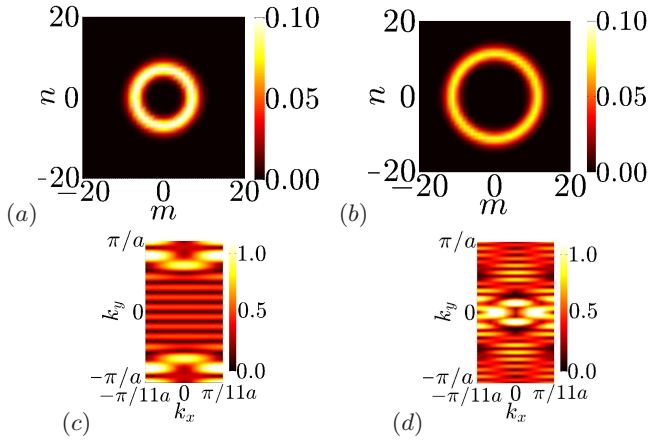

FIG. S1. Supplementary Figure : **Further Examples of Toroidal Landau Levels**. (a)&(b) The wave function, $|\psi(\mathbf{r})|$, in units of a^{-1}. The left (right) figure is the 16th (49th) lowest eigenstate of the Harper-Hofstadter Hamiltonian with a harmonic trap for $\alpha = 1/11$, $\kappa a^2/J = 0.02$ and $N = (133)^2$. (c)&(d) The wave-function, $|\psi(\mathbf{k})|$, in the magnetic Brillouin zone, in units of $(2\pi/\sqrt{N}a)^{-1}$. The left (right) figure is in excellent agreement with the $\beta = 15$ ($\beta = 39$) toroidal Landau level in the lowest band (Eq. 20).

Further examples of toroidal Landau levels are shown in Supplementary Figure 1. These are again in excellent agreement with theoretical toroidal Landau levels (20). The importance of the topology of the space is apparent from a comparison of these states with the usual plane wave basis of Landau levels:

$$\chi_\beta(\mathbf{k}) \propto e^{ik_y y} e^{-(k_x - y l_{\Omega_n}^2)^2/2l_{\Omega_n}^2} H_\beta(k_x/l_{\Omega_n} - y l_{\Omega_n}), \tag{22}$$

where $\mathbf{k}$ varies continuously over infinite momenta and is not constrained to the Brillouin zone. (The Berry connection is again chosen in the Landau gauge specified in the main text). The wave functions of this basis of Landau levels are characterised by a plane wave along k_y, and β nodes along k_x. In the same gauge, the toroidal Landau levels have a markedly different structure (Fig. S1 c & d). The toroidal Landau levels vary along both momenta directions, with the majority of nodes along k_y.

[1] R. Karplus and J. M. Luttinger, Phys. Rev. **95**, 1154 (1954).
[2] D. Xiao, M.-C. Chang, and Q. Niu, Rev. Mod. Phys. **82**, 1959 (2010).
[3] F. Wilczek and A. Zee, Phys. Rev. Lett. **52**, 2111 (1984).
[4] C. N. Yang and R. L. Mills, Phys. Rev. **96**, 191 (1954).
[5] M. Z. Hasan and C. L. Kane, Rev. Mod. Phys. **82**, 3045 (2010).
[6] X.-L. Qi and S.-C. Zhang, Rev. Mod. Phys. **83**, 1057 (2011).
[7] H. M. Price and N. R. Cooper, Phys. Rev. Lett. **111**, 220407 (2013).
[8] F. Dalfovo, S. Giorgini, L. P. Pitaevskii, and S. Stringari, Rev. Mod. Phys. **71**, 463 (1999).
[9] M. Kohmoto, Ann. Phys. **160**, 343 (1985).
[10] M.-C. Chang and Q. Niu, Phys. Rev. Lett. **75**, 1348 (1995).
[11] B. Bernevig and T. Hughes, Topological Insulators and Topological Superconductors (Princeton University Press, 2013).
[12] M. H. Al-Hashimi and U.-J. Wiese, Ann. Phys. **324**, 343 (2009).